

## *Supplementary Material*

# **Wintertime sea surface temperature variability modulated by Arctic Oscillation in the northwestern part of the East/Japan Sea and its relationship with marine heatwaves**

**Se-Yong Song<sup>1</sup>, Yoo-Jun Kim<sup>2</sup>, Eun-Joo Lee<sup>3</sup>, Sang-Wook Yeh<sup>4\*</sup>, Jae-Hun Park<sup>3</sup> and Young-Gyu Park<sup>5</sup>**

<sup>1</sup>Institute of Ocean and Atmospheric Sciences, Hanyang University, ERICA, Ansan, South Korea

<sup>2</sup>Atmosphere and Ocean Research Institute, The University of Tokyo, Kashiwa, Chiba, Japan

<sup>3</sup>Department of Ocean Sciences, Inha University, Incheon, South Korea

<sup>4</sup>Department of Marine Sciences and Convergence Technology, Hanyang University, ERICA, Ansan, South Korea

<sup>5</sup>Ocean Circulation Research Center, Korea Institute of Ocean Science and Technology, Busan 49111, Republic of Korea

### **\* Correspondence:**

Prof. Sang-Wook Yeh

swyeh@hanyang.ac.kr

### **Contents**

Supplementary Figure 1

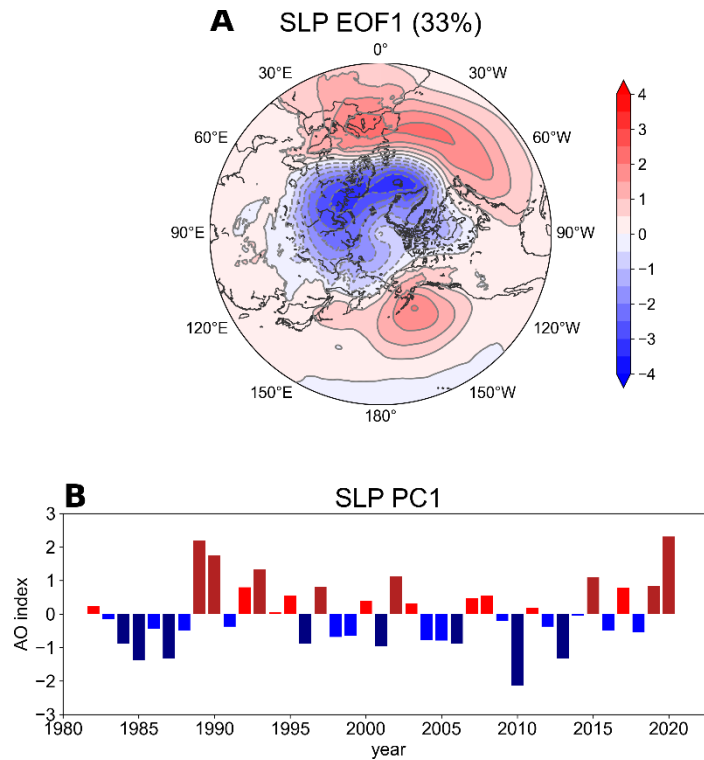
Supplementary Figure 2

Supplementary Figure 3

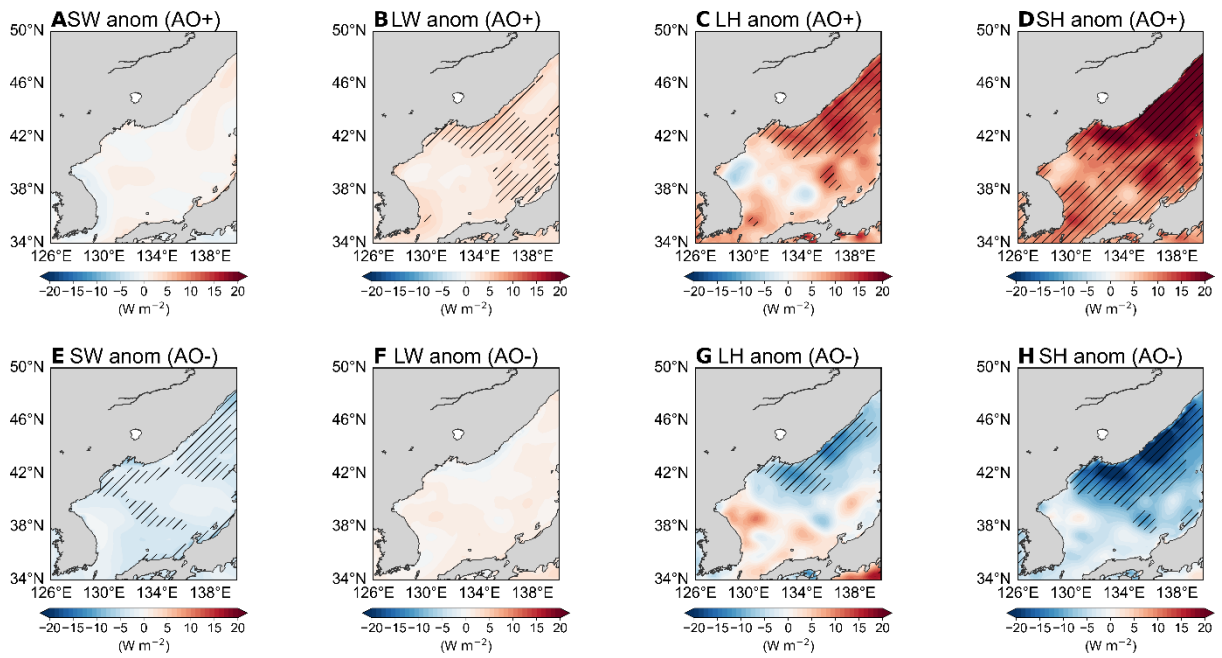
Supplementary Figure 4

Supplementary Figure 5

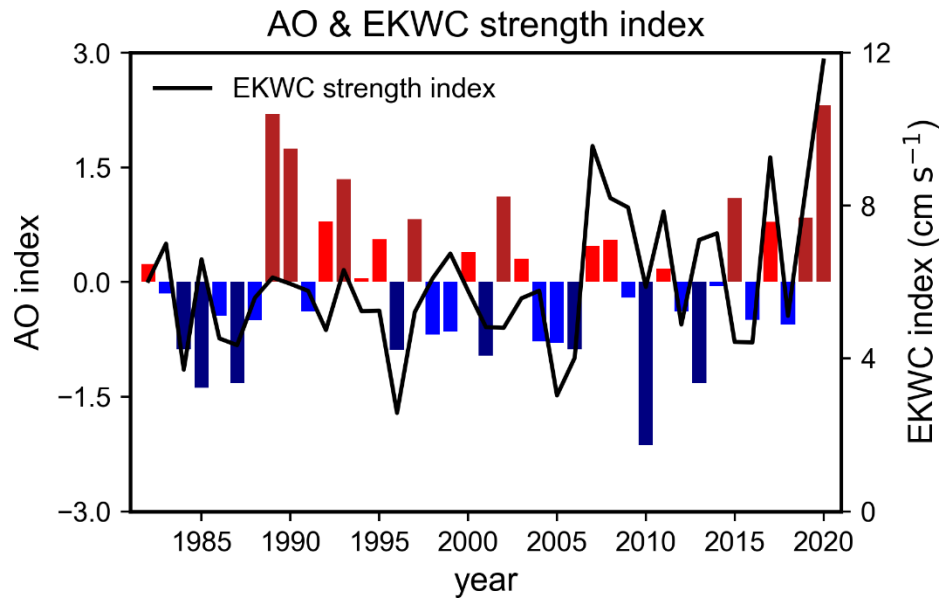
Supplementary Figure 6



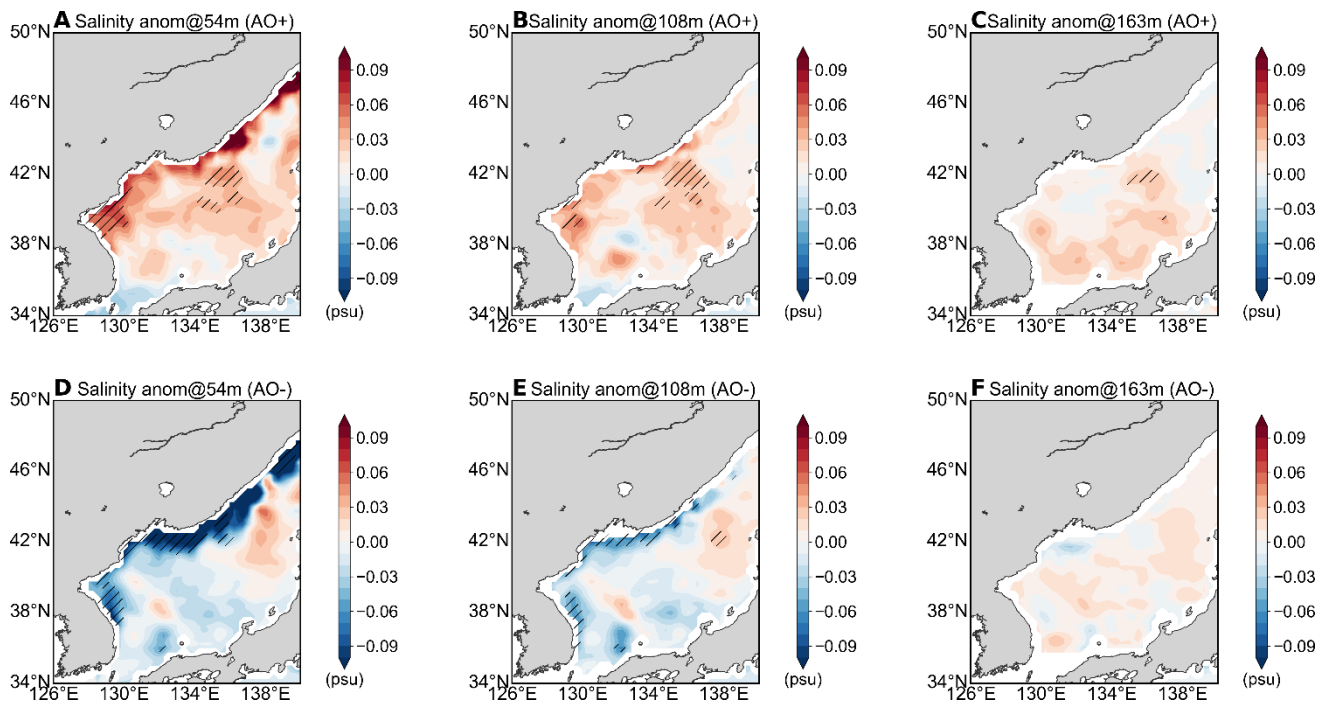
**Supplementary Figure 1.** (A) Spatial pattern and (B) time series for the wintertime (January-February-March, JFM) Arctic Oscillation from 1982 to 2020 based on the fifth generation of the European Centre for Medium-Range Weather Forecast reanalysis product datasets (ERA5). The percentages in (A) indicate the corresponding explained variances. The dark red and blue bars in (B) denote the composite year for the AO positive and negative phases based on 0.8 standard deviations, respectively.



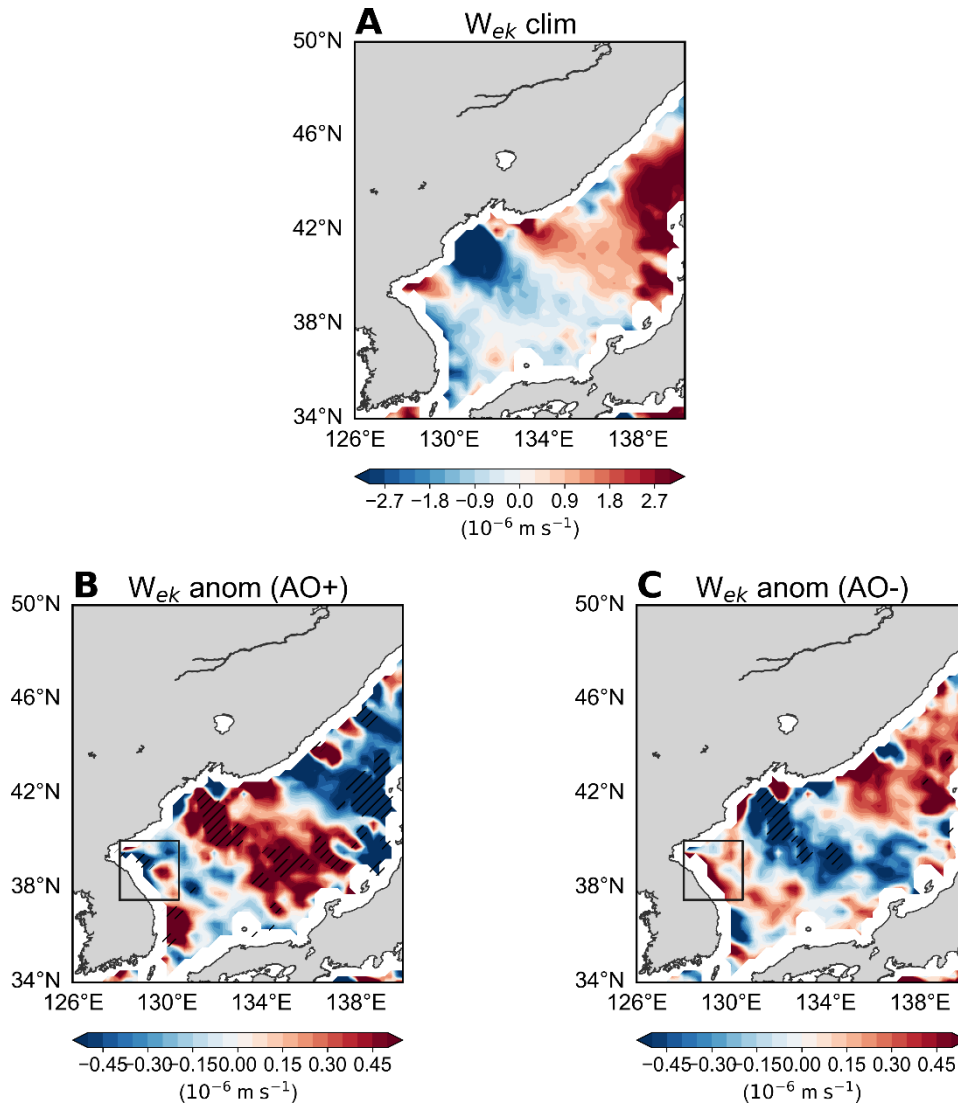
**Supplementary Figure 2.** Composite map of the wintertime air-sea heat flux anomalies (shading,  $\text{W m}^{-2}$ ) as in (A) surface net shortwave radiation (SW), (B) surface net longwave radiation (LW), (C) latent heat flux (LH), and (D) sensible heat flux (SH) based on the AO positive years. (E-H) As in (A-D), but for the AO negative years. Positive (negative) sign denotes that the ocean gains (losses) heat from the atmosphere. The black hatching denotes the values with the statistical significance at the 90% confidence level based on the student's  $t$ -test.



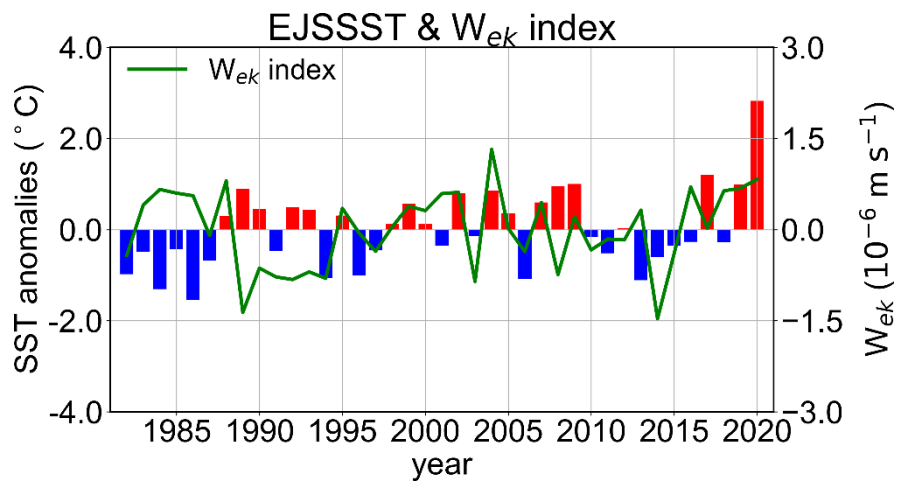
**Supplementary Figure 3.** Time series of the AO (bars, in left y-axis) and the EKWC strength index (black line, in right y-axis), which is defined as the meridional surface current averaged over 129.25°-130.25°E, 35°-38°N.



**Supplementary Figure 4.** Composite map of the wintertime salinity anomalies at (A) 54 m, (B) 108 m, and (C) 163 m based on the AO positive years. (D-F) As in (A-C), but for the AO negative years. The black hatching denotes the values with the statistical significance at the 90% confidence level based on Student's *t*-test.



**Supplementary Figure 5.** Climatological wintertime mean of the (A) Ekman pumping velocity ( $W_{ek}$ ). Positive (negative) sign denotes the Ekman upwelling (downwelling). Composite map of the wintertime  $W_{ek}$  anomalies based on the (B) AO positive and (C) AO negative years. The black hatching denotes the values with a statistical significance at the 90% confidence level based on the student's  $t$ -test. The black box in (B,C) denotes the region where the  $W_{ek}$  anomaly exhibits the distinct signal with respect to the AO phase. Here, the  $W_{ek}$  was calculated as  $\frac{1}{\rho f} \left( \frac{\partial \tau_y}{\partial x} - \frac{\partial \tau_x}{\partial y} \right)$  where  $\rho$  is the seawater density ( $1028 \text{ kg/m}^3$ ),  $f$  is the Coriolis parameter, and  $\tau$  is the wind stress.



**Supplementary Figure 6.** Time series of the EJSSST (bars, in left y-axis) and the  $W_{ek}$  index (green line, in right y-axis), which is defined as the area-weighted average of Ekman pumping velocity in black box of Supplementary Figures 5B,C.